Pharmaceutical Development and Technology, 2013; 18(3): 686–693

ISSN 1083-7450 print/ISSN 1097-9867 online
DOI: 10.3109/10837450.2012.685657

informa
healthcare

RESEARCH ARTICLE

Nanoparticle formation by using shellac and chitosan for a protein delivery system

Pakorn Kraisit[1,2], Sontaya Limmatvapirat[1,2], Jurairat Nunthanid[1,2], Pornsak Sriamornsak[1,2], and Manee Luangtana-anan[1,2]

[1]*Department of Pharmaceutical Technology, Faculty of Pharmacy, Silpakorn University, Nakhon Pathom, Thailand and*
[2]*Pharmaceutical Biopolymer Group (PBiG), Faculty of Pharmacy, Silpakorn University, Nakhon Pathom, Thailand*

Abstract

The potential of using two natural polymers (chitosan and shellac) for the formation of nanoparticles by the process of ionic cross-linking to encapsulate bovine serum albumin, a model protein was investigated. Depending on the concentrations of chitosan, shellac and bovine serum albumin, three physical states – nanoparticle, aggregation, and solution could be observed as a result of the electrostatic force. The formation of nanoparticles was due to the balance between the repulsion force and attractive force while the imbalance between both forces resulted in the formation of aggregation and solution. The Fourier transform infrared spectroscopy and differential scanning calorimetry were applied to prove the nanoparticle formation. The particle size was characterized by the light scattering technique and was found in the range between 100 and 300 nm. The morphology of the particles, detected by transmission electron microscopy was spherical shape. The result showed that the zeta potential of the nanoparticles possessed positive charges. The concentrations of chitosan, shellac and bovine serum albumin had an influence on the physicochemical properties of the nanoparticles such as the particle size, the zeta potential, the encapsulation, the loading efficiencies and the cumulative release. Therefore, chitosan and shellac could be used to form nanoparticles for protein delivery by the ionic cross-linking method.

Keywords: Chitosan, shellac, nanoparticle, protein, polyelectrolyte complexes

Introduction

Nanoparticulate delivery systems have been widely investigated in the pharmaceutical industry due to the ability of controlled release of peptide drugs, the protection from degradation in the GI tract and the enhancement of transmucosal transport leading to an improvement of bioavailability.[1,2] Several techniques have been used for the preparation of nanoparticles for oral delivery system such as the solvent evaporation, the interfacial polymerization and the emulsion polymerization methods. These techniques involve heat, organic solvent and violent agitation processes which are complicated to execute and can be potentially harmful to therapeutic proteins and peptides.[2] Ionic cross-linking is a popular technique due to its simplicity and mild condition. The technique involves the cross-linking between cationic molecules and anionic molecules via electrostatic interaction.[3,4] The most commonly used cationic polymer is chitosan and the anionic material is tripolyphosphate (TPP).

Chitosan, a cationic natural biopolymer, produced from deacetylation of chitin [poly-β-(1-4)-*N*-acetyl-D-glucosamine] which can be extracted from crustaceans, insects, fungi, etc.[5-9] The advantages of using chitosan is biocompatible, biodegradable, low toxicity, good mucoadhesion and membrane permeable enhancing properties by opening of tight epithelial cell junctions.[8,10-12] It is soluble in an acidic solution at pH below 6.4–6.5.[13,14] In addition, the protonation of primary amino groups at lower pH contributes to the positive charges for cross-linking with polyanions especially tripolyphosphate (TPP) to form nanoparticles for drug and protein delivery system.[12,15-18] Several attempts have been made to employ

Address for Correspondence: Manee Luangtana-anan, Department of Pharmaceutical Technology, Faculty of Pharmacy, Silpakorn University, Nakhon Pathom 73000, Thailand. Tel.: +66 34255800. Fax: +66 34255801. E-mail: manee@su.ac.th.
(Received 08 December 2011; revised 21 March 2012; accepted 30 March 2012)

biomaterials possessing polyanions, such as alginate and pectin to replace tripolyohosphate in the formation of nanoparticulate polyelectrolyte complexes.[9,19] The polyelectrolyte complexes were formed by the electrostatic interactions between cationic and anionic polymers to act as the carrier for drug, peptide and protein and gene delivery systems.[9,19-23] In this study, the natural biopolymer, shellac (SH) possessing polyanion instead of TPP was explored. SH produced from lac insect *Laccifer lacca* is abundant in Thailand, China and India. The resinous secretion can be purified to yield SH which has been used in the food industry, paint industry and, in a lesser extent, in the pharmaceutical industry.[24,25] SH begins to dissolve above pH 7.0 (the pKa of SH is 6.9–7.5) which can provide an advantage to be used in the pH of the body fluid (pH 7.4).[26] The main structure of SH is the combination of polyesters and single esters consisting of hydroxyl and carboxyl groups as shown in Figure 1.[24] Hence, SH possesses the ability to deprotonate in the alkaline solutions to give polyanions favorable for the formation of polyelectrolyte complexes with chitosan. In this study, both chitosan and SH were used in salt forms. SH was used in ammonium salt form due to its better stability and aqueous solubility while chitosan glutamate (CG) is soluble over a broad pH range in the intestinal tract and is convenient to handle.[27,28] CG was prepared by the spray drying technique from the chitosan base. The lower molecular weight of 35 kDa of CG was chosen because the nano size range could be obtained.[15]

The concentrations of the cationic and anionic polymers exerted a significant influence on the formation and the physical properties of the nanoparticles such as the size, zeta potential, encapsulation and release of drugs or proteins.[7,10,12] Pan et al. demonstrated that nanoparticles could be formed at an optimum concentrations of chitosan and TPP, i.e. in the range of 0.9–3.0 mg/mL and 0.3–0.8 mg/mL, respectively.[29] A similar result using cyclodextrin to form nanoparticles with the aid of chitosan and TPP was reported.[30] Therefore, the effect of the concentrations of CG and SH on the formation of nanoparticles for the encapsulation of bovine serum albumin (BSA, a model protein) in oral drug delivery system was investigated. FT-IR and DSC were used to prove the interaction among CG, SH and BSA. Additionally, BSA-loaded chitosan–shellac nanoparticles were characterized in terms of the particle size, zeta potential, morphology, encapsulation efficiency (EE), loading efficiency (LE) and *in vitro* BSA release.

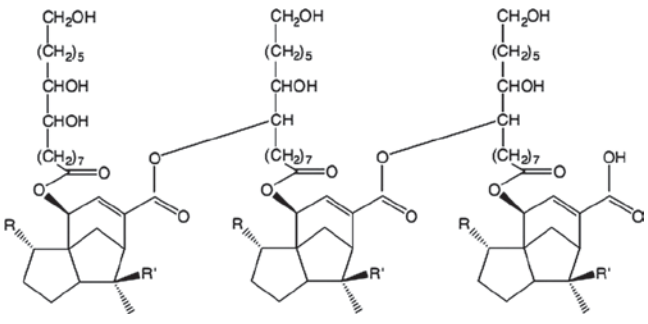

Figure 1. Chemical structure of shellac.

Materials and methods

Materials

Chitosan, with a molecular weight of 35 kDa and 85% degree of deacetylation, was obtained from Seafresh Chitosan Lab. Co (Bangkok, Thailand), and the SH was obtained from Thananchai Part., Ltd. (Bangkok, Thailand). BSA was purchased from Sigma (Germany), and glutamic acid was from Fluka (Switzerland). All the other reagents were of analytical grade.

Preparation of chitosan glutamate

CG was prepared by dissolving the chitosan base in glutamic acid solution. The molar ratio of glucosamine and glutamic acid was 1:1 mole. In order to avoid excess glutamic acid, minimum amount of glutamic acid was used to give an exact clear solution. The solution was adjusted to 2000 g with distilled water to make a 1% w/w solution, and was stirred for 12 h. The solution was spray-dried (Labplant Spray Dryer, SD-06, UK) with an inlet temperature of 130°C and a spraying rate of 5 mL/min. [15]

Preparation of the shellac solution

The SH solution was prepared by dissolving SH in ammonium hydroxide solution. The amount of ammonium hydroxide solution added was based on the calculation of the acid value of the SH according to our previous report. [24] The solutions were stirred overnight.

Preparation of BSA-loaded chitosan–shellac nanoparticles

BSA-loaded chitosan–shellac nanoparticles were prepared by ionic cross-linking between the cationic molecules of chitosan and the anionic molecules of SH for encapsulation of BSA as a model protein. The concentrations of CG were in the range 0.090–0.110% w/v while those of SH were 0.030–0.070% w/v and the BSA concentrations were 1.0, 1.5 and 2.0 mg/mL. The BSA was mixed with the CG solution for 5 min and the SH was then added drop-wise. The colloidal solution was further stirred for 30 min. The effect of the concentrations of CG and SH was investigated for the fixed concentrations of SH and CG at 0.050 and 0.100% w/v, respectively. BSA-loaded chitosan–shellac nanoparticles were characterized in terms of their zeta potential, particle size, BSA encapsulation efficiency and BSA loading efficiency.

Physicochemical characterization of BSA-loaded chitosan–shellac nanoparticles

The nanoparticles were characterized in terms of their sizes using the light scattering technique (Horiba, LA-950, Kyoto, Japan), and the zeta potential was measured by the Zeta Plus (Brookhaven Instruments Co., New York, NY, USA). All measurements were carried out in triplicate.

Morphological examination of the nanoparticles was performed by a transmission electron microscope (TEM, TEM-1230, JEOL, Japan). One drop of the sample was placed on a copper grid, adsorbed with a filter paper and air-dried for 20 min, prior to the morphology study.

Fourier transform infrared spectroscopy

Fourier transformed infrared (FT-IR) spectroscopy was used to characterize the BSA-loaded chitosan–shellac nanoparticles and to confirm the ionic cross-linking between the cationic molecules of chitosan and the anionic molecules of SH. The nanoparticles were separated from the colloidal solution by high speed centrifugation at 11,000 rpm at 25°C for 10 min (Universal 320 R, Germany). The supernatant from the centrifugation was decanted and the precipitated nanoparticles were dried in a vacuum freezer at –50°C for 18 h. The nanoparticles were pulverized, blended with KBr, and compressed for the measurement using a FT-IR spectrophotometer (Nicolet, Magna 750, USA).

Differential scanning calorimetry

Differential scanning calorimetry (DSC) thermograms of BSA-loaded chitosan–shellac nanoparticles were measured by using a DSC (DSC 7, Perkin-Elmer, USA). 2–4 mg of sample was accurately weighed onto a solid aluminum pan, and sealed. The measurement was performed between 25 and 300°C under the purging of nitrogen gas at a heating rate of 10°C/min.

Evaluation of BSA encapsulation and loading efficiencies

The BSA-loaded chitosan–shellac nanoparticles were separated from the colloidal solution by high speed centrifugation at 11,000 rpm at 25°C for 10 min. The free BSA content from the supernatant was analyzed by a UV spectrophotometer (Lambda 2, Perkin-Elmer, Germany) at 550 nm using the Lowry method. Triplicate samples were analyzed and the EE and LE were calculated using equations 1 and 2, respectively.

$$\%EE = \frac{\text{Total amount of BSA free amount of BSA from supernatant}}{\text{Total amount of BSA}} \times 100 \quad (1)$$

$$\%LE = \frac{\text{Total amount of BSA free amount of BSA from supernatant}}{\text{Nanoparticle weight}} \times 100 \quad (2)$$

Evaluation of BSA release

Five millliter of the BSA-loaded chitosan–shellac nanoparticles was placed in a 50 mL bottle, and 10 mL of a 0.1 M phosphate buffer solution (PBS) at pH 7.4 was added. The colloidal solution was shaken at 150 rpm, and incubated at 37°C. At proper time intervals, a sample was removed, and the same amount of PBS was added. High speed centrifugation at 11,000 rpm and 25°C for 10 min was conducted to separate the nanoparticles. Triplicate samples of free BSA content from the supernatant were analyzed by using the Lowry method.[15]

Statistical analysis

Each data was expressed as mean ± standard deviation (SD) of three determinations (n = 3). An analysis of variance (ANOVA) was carried out to find out the statistical analysis of EE, LE and BSA release at the 0.05 significant levels.

Results and discussion

Physicochemical characterizations of BSA-loaded chitosan–shellac nanoparticles

The two biopolymers were used to prepare nanoparticles for protein delivery systems by the ionic cross-linking technique. Table 1 shows the effect of various concentrations of CG, SH and BSA on their particle sizes and zeta potential. Depending on the concentrations of CG, SH and BSA, there were three physical states; nanoparticle, aggregation and solution.[29, 30] The particle size of the colloid was in 100–300 nm size range. For 1 mg/mL of BSA, at various concentrations of SH, the nanoparticles could not be formed, and only a clear solution was obtained. This proved that the formation was concentration dependence. The zeta potentials of all nanoparticles displayed a positive charge. The positive charge of the nanoparticles was attributed to the unoccupied amine groups of the chitosan. The increase in the concentration of CG at the fixed concentration of SH, the higher zeta potential was obtained[8] because of the increase in the positive charge from the amine groups of chitosan. However, the increase in the negative charge of SH did not result in the reduction of the zeta potential, which was not in agreement with the use of tripolyphosphate (TPP) as polyanion to form nanoparticles.[7] The increase in the zeta potential with the increase in the concentration of SH was attributed to the increase in the unoccupied amine group of CG due to the competitiveness of deprotonated carboxylic groups between SH and BSA and the large molecule of SH. These were attributed to the difficulty in interaction with amine group of chitosan. The addition of BSA caused the reduction in the zeta potential and the higher BSA concentrations showed the higher decrease in the zeta potential.[31] The result proved that the BSA showed a negative charge as the pH being studied was higher than the pI value (pI = 4.7, the pH under this condition was approximately 5.5). There was the electrostatic interaction between NH3+ from the chitosan and the negative charge from the BSA. The result was in agreement with the reports of Boonsongrit et al. and Chen et.al.[7,32] They found that the zeta potential decreased with the increase in the BSA concentration resulting from the increased negative charge of BSA. Figure 2 shows the state of

Table 1. Effect of different concentrations of CG, SH and BSA on particle size and zeta potential of BSA-loaded chitosan-shellac nanoparticles (mean ± SD, $n = 3$).

	With BSA (mg/mL)					
	Particle size (nm)			Zeta potential (mV)		
	1.0	1.5	2.0	1.0	1.5	2.0
*Chitosan glutamate concentrations (%w/v)						
0.090	107.3 ± 2.5	280.0 ± 18.2	Ag	30.7 ± 0.7	26.1 ± 1.1	Ag
0.095	145.7 ± 10.7	118.3 ± 2.1	Ag	34.0 ± 0.6	24.2 ± 0.6	Ag
0.100	Sol	104.3 ± 1.2	169.0 ± 4.2	Sol	25.4 ± 0.6	23.7 ± 0.5
0.105	Sol	133.3 ± 0.6	115.3 ± 4.2	Sol	31.5 ± 0.9	27.3 ± 0.7
0.110	Sol	144.0 ± 4.2	102.0 ± 2.0	Sol	37.0 ± 0.8	33.4 ± 1.0
**Shellac concentrations (%w/v)						
0.030	Sol	Sol	135.7 ± 2.1	Sol	Sol	14.5 ± 1.0
0.040	Sol	Sol	173.0 ± 6.7	Sol	Sol	18.1 ± 2.4
0.050	Sol	104.3 ± 1.2	169.0 ± 4.2	Sol	25.4 ± 0.6	23.7 ± 0.5
0.060	Sol	111.3 ± 17.9	144.0 ± 5.2	Sol	32.3 ± 0.4	28.9 ± 0.4
0.070	Sol	145.0 ± 9.9	106.3 ± 1.5	Sol	34.8 ± 0.7	29.1 ± 0.6

*The concentration of SH was fixed at 0.050 % w/v.
**The concentration of CG was fixed at 0.100 % w/v.
Ag, aggregation state; Sol, solution state.

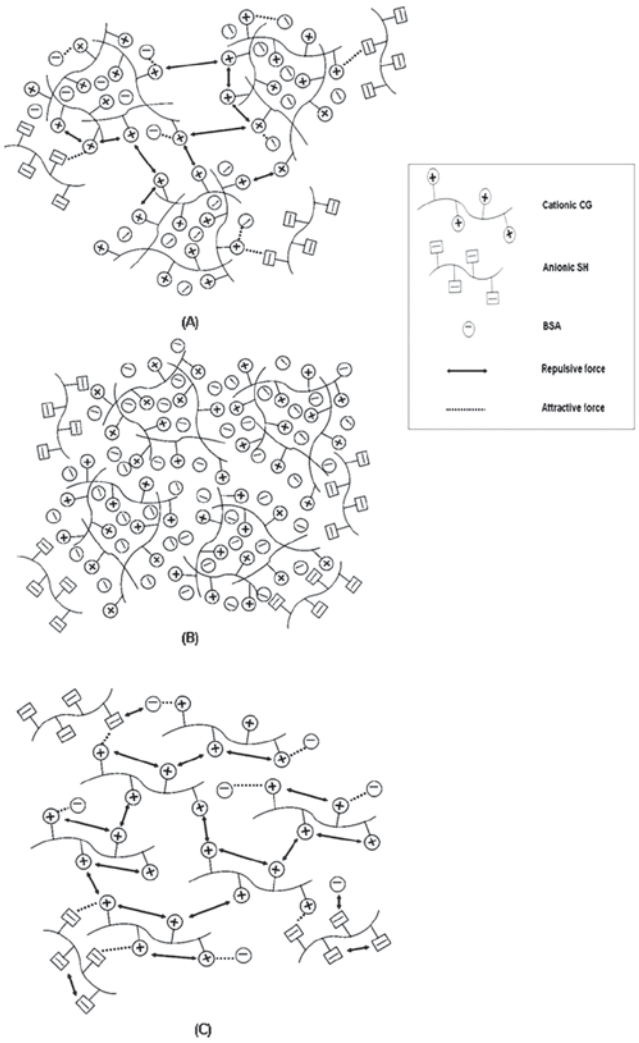

Figure 2. Schematic representation of ionic interaction of nanoparticulate formation (A), aggregation (B) and solution state (C), respectively.

interaction of SH, CG and BSA. They were the formation of the nanoparticles (A), aggregation (B) and solution (C). Figure 2A shows the formation of the nanoparticles due to the ionic interaction between the positive charge of chitosan and the negative charge of BSA and SH. The effect of other ions from glutamate and ammonium ions had little influence on the state of interaction owing to the exact calculation of the amount of glutamic acid and ammonium hydroxide solution used for the preparation of chitosan and SH solutions as described above. The optimum concentrations of CG, SH and BSA contributed to the balance between the attractive force and repulsive force from the anionic and cationic molecules leading to the formation of the nanoparticles. The charge of the nanoparticles attributing to the stability of colloids was reported.[2,10] The high positive charge of the nanoparticles gave the high repulsive force, causing the individual nanoparticles. In this study, the zeta potential of the nanoparticles was in the range of 14–37 as shown in Table 1. The reduction in the zeta potential of the nanoparticles caused the nanoparticles to come closer until it was aggregated. In addition, the pH value played a role on the formation of the particles as previously described.[4,8,10] The increase in the pH led to the reduction in the degree of protonation of the chitosan, and hence the decrease in the zeta potential. This caused the decrease in the electrostatic repulsion force between the particles leading to the aggregated particles as shown in Figure 2B.[8,10] The aggregation was reported and was in accordance with the increase in the pH with the increase in the BSA from 1.5 mg to 2 mg/mL; at 0.090–0.095 %w/v concentration of CG (data was not shown). Figure 2C shows the solution state indicating that each molecule of CG, SH and BSA was apart. This could be due to the greater repulsive force than the attractive force at the lower BSA concentration. This caused the higher unoccupied amine group of

chitosan and the higher zeta potential and hence the solution state was formed.

In order to confirm the morphological characteristic of the BSA-loaded chitosan–shellac nanoparticles, TEM was used as shown in Figure 3. The spherical shape of the nanoparticles was observed. This result could be confirmed that the nanoparticle was formed by using CG and SH for the encapsulation of BSA. The FT-IR spectra of SH, BSA, CG, BSA-loaded chitosan–shellac nanoparticles and physical mixture are shown in Figure 4. All spectra displayed a broad band at 3000–3600 cm^{-1}, indicating the overlap of OH and NH stretchings in the same region.[5,16] In this region, CG and physical mixture were shown in the same peak at 3442 cm^{-1}. In addition, this result was in line with the previous study as the peak of the nanoparticles was shifted to 3312 cm^{-1}, indicating the hydrogen bonding formation.[17] In addition, the FT-IR spectrum of CG shows a peak due to the amide stretching at 1633 cm^{-1} and a strong protonated amino peak at 1564 cm^{-1}.[4] The spectrum of the nanoparticles was shifted from 1633 to 1660 cm^{-1} and the sharp peak was found due to the ionic interaction between the amine group of chitosan and the hydroxyl group of BSA, supporting the formation of the nanoparticles.[27] In addition, the FT-IR bands at 1660 and 1539 cm^{-1} of the nanoparticles were assigned to the amide I and amide II bands, respectively, which are the characteristic of protein spectra,[4] supporting the presence of BSA within the nanoparticles. The bands at 1559 and 1386 cm^{-1} were also assigned to the symmetric and asymmetric carbonyl stretchings of the carboxylate of SH, respectively.[24] This was slightly shifted in the spectrum of the nanoparticles at 1394 cm^{-1}, and the peak at 1559 cm^{-1} of SH was hardly visible in the spectrum of the nanoparticles. However, the peak at 1255 cm^{-1} of SH[25] associated with the carbonyl stretching could also be observed in the spectrum of the physical mixture while this peak of the nanoparticles was shifted to 1249 cm^{-1}, indicating that SH was part of the formation of the nanoparticles. To confirm the results of the formation of protein-loaded nanoparticles, DSC was used to confirm the formation of protein-loaded nanoparticles. The DSC thermograms of SH, BSA, CG, BSA-loaded chitosan–shellac nanoparticles and physical mixture are shown in Figure 5. The DSC thermograms of all substances showed the endothermic peaks around 40–120°C which were associated with the loss of water. The CG showed the endothermic peak at 170.5°C, indicating the glutamate of chitosan.[33] The physical mixture was reported at the same peak but it was not found for the nanoparticles. In addition, the thermogram of BSA showed the decomposition peak at 219.2°C while the peak of the nanoparticles shifted to 223.1°C[4,34]

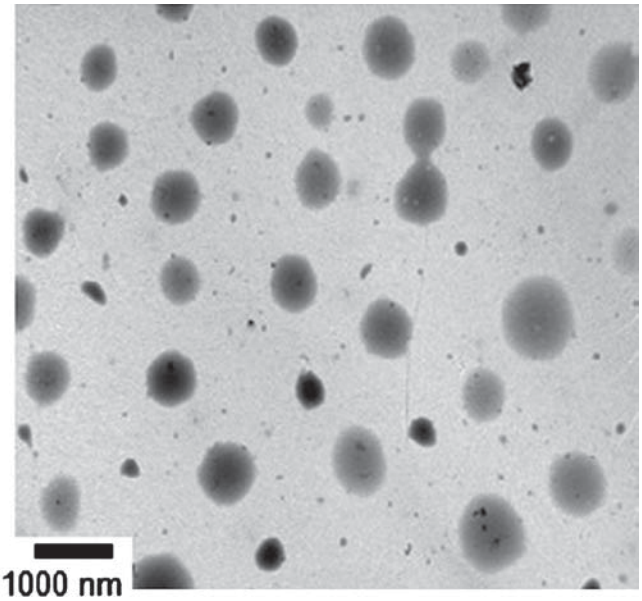

Figure 3. TEM photographs of BSA-loaded chitosan–shellac nanoparticles (CG 0.100 %w/v, SH 0.050 %w/v and BSA 1.50 mg/mL).

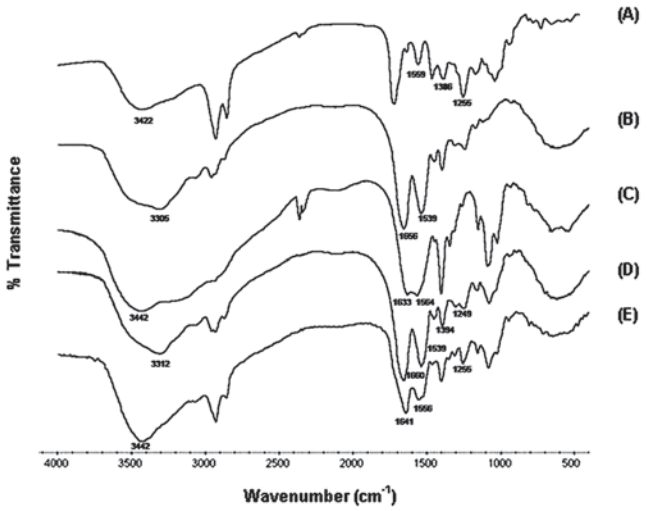

Figure 4. FT-IR spectra of (A) SH, (B) BSA, (C) CG, (D) BSA-loaded chitosan–shellac nanoparticles of CG 0.100 %w/v, SH 0.050 %w/v and BSA 1.5 mg/mL and (E) CG/SH/BSA physical mixture 1:1:1.

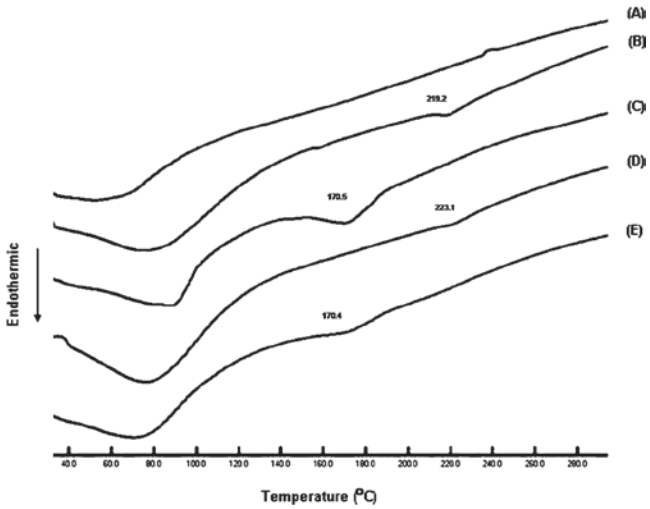

Figure 5. DSC thermograms of (A) SH, (B) BSA, (C) CG, (D) BSA-loaded chitosan–shellac nanoparticles of CG 0.100 %w/v, SH 0.050 %w/v and BSA 1.5 mg/mL and (E) CG/ SH/BSA physical mixture 1:1:1.

as a result of the interaction between each material for the formation of nanoparticle. Therefore, it proved that the formation of nanoparticles could be achieved by the application of two naturally opposite charged polymers for the encapsulation of BSA.

Evaluation of BSA encapsulation and loading efficiencies

Table 2 shows the effect of the concentrations of CG, SH and BSA on EE and LE of BSA-loaded nanoparticles. The EE and LE were in the range of 11–67% and 7–45%, respectively. The increase in the concentrations of CG resulted in the significant ($p < 0.05$) decrease in the EE and LE, which was in an agreement with the other report.[12] This could be the result of the increase in the viscosity which was correlated with the fact that the increase in the concentrations made it difficult for the encapsulation to take place by averting the BSA molecular movement around the chitosan molecule chain.[12, 35] The decrease in EE and LE was consistent with the increase in the zeta potential indicating the higher unoccupied amine of CG with the increase in CG. The higher amount of BSA had a tendency to increase in the EE and LE which was similar to the work of Gan and Wang [12] whereas the opposite effect was reported by other studies.[17, 29] The higher in EE and LE as the increase in BSA was also in accordance with the reduction in the zeta potential confirming that there was an interaction between the positive charge of CG and the negative charge of BSA. The result of varying concentration of SH on the change in EE and LE at the concentration of 1.5 mg/mL BSA showed similar result to varying concentration of CG, and was related to the change in the zeta potential. The decrease in EE and LE was significant ($p < 0.05$) with the increase in SH. Nevertheless, at the concentration of 2.0 mg/mL, the reduction in EE and LE did not change in the same manner as the concentration of 1.5 mg/mL, and the highest EE was obtained for the SH concentration of 0.050%. The EE and LE increased from 22.2 to 57.6% and 16.2 to 41.4%, respectively when SH increased from 0.040 to 0.050 %w/v. Therefore, it could be concluded that the formation of BSA-loaded nanoparticles was only possible for some specific concentrations of the positively charged CG and the negatively charged SH. The optimum concentration of CG, SH and BSA was 0.100, 0.050 %w/v and 2.0 mg/mL, respectively.

Evaluation of BSA release

Release profiles of many reports have exhibited, initially, the burst release of drugs or proteins from the micro or nanoparticles followed by a slow release.[15-17, 29] The mechanism of the release involved two different states; the fast release from the location of the drug on the surface led to the immediate release when it was exposed to the dissolution medium. The next step was the diffusion through the nanoparticles which was the predominant release mechanism.[16] The amount of release was controlled by the EE and the mechanism of encapsulation as presented in Figure 6. The nanoparticles showed the immediate release of BSA from the matrix of all systems, and the amount of release was between 64.3 and 78.1% significantly depending on the concentrations of CG ($p < 0.05$). After 30 min, a gradual and slow release was reported. The immediate release was due to the part of adsorbed BSA at the surface and the competitiveness between phosphate ion and the anion of BSA at the binding sites.[18,36] The CG concentrations affected the total release of BSA from the nanoparticles. It decreased from 87.0 to 73.4% with the increasing CG concentration from 0.095 to 0.105% w/v ($p < 0.05$), which was in agreement with the work of Gan and Wang;[12] however, it was contrast to the report of Xu and Du.[17] The lowest release was found for 0.105%w/v CG as a result of the lowest encapsulation.

Table 2. Effect of different concentrations of CG, SH and BSA on encapsulation efficiency (EE) and loading efficiency (LE) of BSA-loaded chitosan-shellac nanoparticles (mean ± SD, $n = 3$).

	With BSA (mg/ml)					
	Encapsulation efficiency (%)			Loading efficiency (%)		
	1.0	1.5	2.0	1.0	1.5	2.0
*Chitosan glutamate concentrations (%w/v)						
0.090	29.7 ± 1.0	67.4 ± 3.9	Ag	17.3 ± 0.6	45.6 ± 2.6	Ag
0.095	21.2 ± 1.1	49.2 ± 1.0	Ag	12.1 ± 0.7	32.8 ± 0.7	Ag
0.100	Sol	22.8 ± 0.5	57.6 ± 0.2	Sol	15.0 ± 0.3	41.4 ± 0.1
0.105	Sol	13.9 ± 0.5	37.6 ± 3.1	Sol	9.0 ± 0.3	26.8 ± 2.2
0.110	Sol	13.5 ± 0.7	20.4 ± 0.3	Sol	8.6 ± 0.4	14.4 ± 0.2
**Shellac concentrations (%w/v)						
0.030	Sol	Sol	26.2 ± 0.4	Sol	Sol	19.3 ± 0.3
0.040	Sol	Sol	22.2 ± 0.1	Sol	Sol	16.2 ± 0.1
0.050	Sol	22.8 ± 0.5	57.6 ± 0.2	Sol	15.0 ± 0.3	41.4 ± 0.1
0.060	Sol	16.3 ± 0.3	34.8 ± 1.5	Sol	10.6 ± 0.2	24.8 ± 1.1
0.070	Sol	11.9 ± 0.2	27.4 ± 0.7	Sol	7.6 ± 0.1	19.3 ± 0.5

*The concentration of SH was fixed at 0.050 % w/v.
**The concentration of CG was fixed at 0.100 % w/v.
Ag, aggregation state; Sol, solution state.

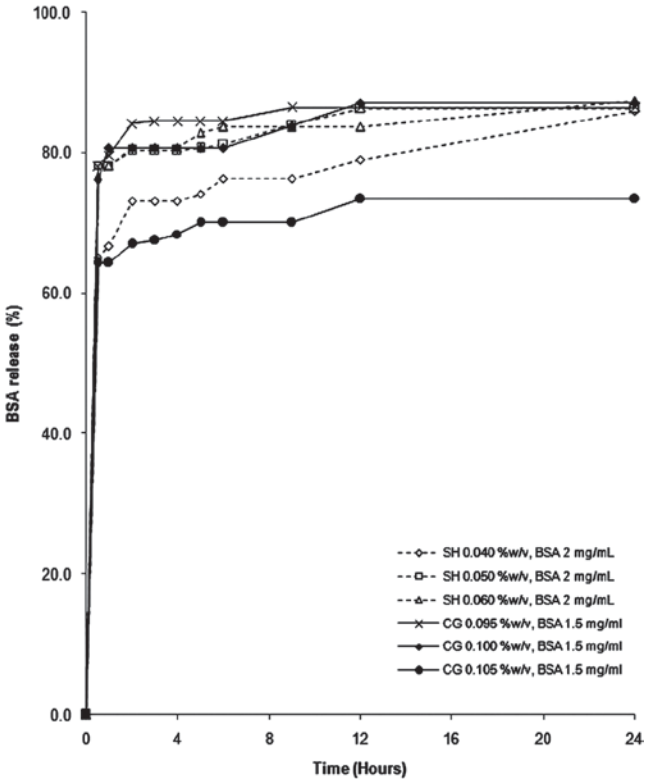

Figure 6. The release profile of BSA-loaded chitosan-shellac nanoparticles at different concentrations of CG and SH in phosphate buffer solution at pH 7.4, 37°C (mean SD, $n = 3$).

The higher levels of encapsulated BSA tended to have an initially higher diffusion rate contributing to a higher driving gradient. In addition, the lower release was in accordance with the larger size. The larger size at 0.105% w/v CG attributed to the larger diffusion path length for the BSA and the lower contact surface area of the larger particles with the dissolution medium.[3] Hence, the release of 0.105 %w/v CG was lower as a result of the larger particle size and the lower EE. The cumulative amounts of BSA released from the various concentrations of SH were around 85–87%w/v, the release did not differ significantly ($p > 0.05$), and showed the burst release initially. The release of BSA at 0.040 %w/v SH was lower than the others ($p < 0.05$), due to the lower EE and the larger size. The cumulative amount of BSA did not release completely due to the entrapment of BSA within the matrix of the nanoparticles, which was in agreement with other studies.[12, 18] In addition, the extended release over a longer time period until 48 h was performed; the result did not significantly differ from the result of 24 h. (Data was not shown) The stability of protein after the release was also performed by gel electrophoresis. The result showed that there was no conformation change after the release and the process of release did not affect the stability of protein. Therefore, it could be concluded that the release of BSA from the particulate systems was dependent on the size and the EE.

Conclusions

The nanoparticles could be prepared by ionic cross-linking between CG and SH to encapsulate BSA. The optimum concentrations of CG, SH and BSA played an important role in the formation of the nanoparticles. The mechanism of formation of the nanoparticles or aggregation or solution state could be described by the electrostatic force of the positive and negative charges. The EE, LE and the cumulative release of BSA could be modified depending on the concentrations of CG, SH and BSA. In summary, SH could be applied as natural polyanion for polyelectrolyte complex. CG and SH, the natural polymers, are potentially useful polymers for the nanoparticulate carrier as protein and drug delivery systems.

Acknowledgments

The authors wish to thank the Thailand Research Fund for the financial support. In addition, the authors would like to thank Assoc. Prof. Dr. Surachai Nimgirawath for the proof reading of the manuscript.

Declaration of interest

Financial support was received from the Thailand Research Fund through the Royal Golden Jubilee Ph.D. Program (Grant No.PHD/0112/2549). The authors report no conflicts of interest. The authors alone are responsible for the content and writing of the paper.

References

1. Chen F, Zhang ZR, Yuan F, Qin X, Wang M, Huang Y. *In vitro* and *in vivo* study of N-trimethyl chitosan nanoparticles for oral protein delivery. Int J Pharm 2008;349:226–233.
2. Sun W, Mao S, Mei D, Kissel T. Self-assembled polyelectrolyte nanocomplexes between chitosan derivatives and enoxaparin. Eur J Pharm Biopharm 2008;69:417–425.
3. Agnihotri SA, Mallikarjuna NN, Aminabhavi TM. Recent advances on chitosan-based micro- and nanoparticles in drug delivery. J Control Release 2004;100:5–28.
4. Sarmento B, Ferreira D, Veiga F, Ribeiro AN. Characterization of insulin-loaded alginate nanoparticles produced by ionotropic pre-gelation through DSC and FTIR studies. Carbohydr Polymers 2006;66:1–7.
5. Nunthanid J, Laungtana-Anan M, Sriamornsak P, Limmatvapirat S, Puttipipatkhachorn S, Lim LY et al. Characterization of chitosan acetate as a binder for sustained release tablets. J Control Release 2004;99:15–26.
6. Bernkop-Schnürch A. Chitosan and its derivatives: potential excipients for peroral peptide delivery systems. Int J Pharm 2000;194:1–13.
7. Boonsongrit Y, Mitrevej A, Mueller BW. Chitosan drug binding by ionic interaction. Eur J Pharm Biopharm 2006;62:267–274.
8. de Moura MR, Aouada FA, Mattoso LH. Preparation of chitosan nanoparticles using methacrylic acid. J Colloid Interface Sci 2008;321:477–483.
9. Sarmento B, Ribeiro A, Veiga F, Sampaio P, Neufeld R, Ferreira D. Alginate/chitosan nanoparticles are effective for oral insulin delivery. Pharm Res 2007;24:2198–2206.
10. Gan Q, Wang T, Cochrane C, McCarron P. Modulation of surface charge, particle size and morphological properties of chitosan-TPP

nanoparticles intended for gene delivery. Colloids Surf B Biointerfaces 2005;44:65–73.
11. de Britto D, de Assis OB. Synthesis and mechanical properties of quaternary salts of chitosan-based films for food application. Int J Biol Macromol 2007;41:198–203.
12. Gan Q, Wang T. Chitosan nanoparticle as protein delivery carrier–systematic examination of fabrication conditions for efficient loading and release. Colloids Surf B Biointerfaces 2007;59:24–34.
13. Lameiro MH, Lopes A, Martins LO, Alves PM, Melo E. Incorporation of a model protein into chitosan-bile salt microparticles. Int J Pharm 2006;312:119–130.
14. Hyung Park J, Kwon S, Lee M, Chung H, Kim JH, Kim YS et al. Self-assembled nanoparticles based on glycol chitosan bearing hydrophobic moieties as carriers for doxorubicin: *in vivo* biodistribution and anti-tumor activity. Biomaterials 2006;27:119–126.
15. Luangtana-anan M, Opanasopit P, Ngawhirunpat T, Nunthanid J, Sriamornsak P, Limmatvapirat S et al. Effect of chitosan salts and molecular weight on a nanoparticulate carrier for therapeutic protein. Pharm Dev Technol 2005;10:189–196.
16. Papadimitriou S, Bikiaris D, Avgoustakis K, Karavas E, Georgarakis M. Chitosan nanoparticles loaded with dorzolamide and pramipexole. Carbohydr Polymers 2008;73:44–54.
17. Xu Y, Du Y. Effect of molecular structure of chitosan on protein delivery properties of chitosan nanoparticles. Int J Pharm 2003; 250:215–226.
18. Xu Y, Du Y, Huang R, Gao L. Preparation and modification of N-(2-hydroxyl) propyl-3-trimethyl ammonium chitosan chloride nanoparticle as a protein carrier. Biomaterials 2003;24:5015–5022.
19. George M, Abraham TE. Polyionic hydrocolloids for the intestinal delivery of protein drugs: alginate and chitosan–a review. J Control Release 2006;114:1–14.
20. Argin-Soysal S, Kofinas P, Lo YM. Effect of complexation conditions on xanthan-chitosan polyelectrolyte complex gels. Food Hydrocolloids 2009;23:202–209.
21. Cafaggi S, Russo E, Stefani R, Leardi R, Caviglioli G, Parodi B et al. Preparation and evaluation of nanoparticles made of chitosan or N-trimethyl chitosan and a cisplatin-alginate complex. J Control Release 2007;121:110–123.
22. Gazori T, Khoshayand MR, Azizi E, Yazdizade P, Nomani A, Haririan I. Evaluation of Alginate/Chitosan nanoparticles as antisense delivery vector: Formulation, optimization and in vitro characterization. Carbohydrate Polymers 2009;77:599–606.
23. Zheng Y, Yang W, Wang C, Hu J, Fu S, Dong L et al. Nanoparticles based on the complex of chitosan and polyaspartic acid sodium salt: preparation, characterization and the use for 5-fluorouracil delivery. Eur J Pharm Biopharm 2007;67:621–631.
24. Limmatvapirat S, Limmatvapirat C, Puttipipatkhachorn S, Nuntanid J, Luangtana-Anan M. Enhanced enteric properties and stability of shellac films through composite salts formation. Eur J Pharm Biopharm 2007;67:690–698.
25. Limmatvapirat S, Panchapornpon D, Limmatvapirat C, Nunthanid J, Luangtana-Anan M, Puttipipatkhachorn S. Formation of shellac succinate having improved enteric film properties through dry media reaction. Eur J Pharm Biopharm 2008;70:335–344.
26. Limmatvapirat S, Limmatvapirat C, Luangtana-Anan M, Nunthanid J, Oguchi T, Tozuka Y et al. Modification of physicochemical and mechanical properties of shellac by partial hydrolysis. Int J Pharm 2004;278:41–49.
27. Specht F, Saugestad M, Waaler T, Miller BW. The application of shellac as an acidic polymer for enteric coating. Pharmaceut Tech 1998;10:20–28.
28. Limmatvapirat S, Nunthanid J, Luangtana-anan M, Puttipipatkhachorn S. Effect of alkali treatment on properties of native shellac and stability of hydrolyzed shellac. Pharm Dev Technol 2005;10:41–46.
29. Pan Y, Li YJ, Zhao HY, Zheng JM, Xu H, Wei G et al. Bioadhesive polysaccharide in protein delivery system: chitosan nanoparticles improve the intestinal absorption of insulin in vivo. Int J Pharm 2002;249:139–147.
30. Krauland AH, Alonso MJ. Chitosan/cyclodextrin nanoparticles as macromolecular drug delivery system. Int J Pharm 2007;340:134–142.
31. Luangtana-Anan M, Limmatvapirat S, Nunthanid J, Chalongsuk R, Yamamoto K. Polyethylene glycol on stability of chitosan microparticulate carrier for protein. AAPS PharmSciTech 2010;11:1376–1382.
32. Chen F, Zhang ZR, Huang Y. Evaluation and modification of N-trimethyl chitosan chloride nanoparticles as protein carriers. Int J Pharm 2007;336:166–173.
33. Portero A, Remunán-López C, Vila-Jato JL. Effect of chitosan and chitosan glutamate enhancing the dissolution properties of the poorly water soluble drug nifedipine. Int J Pharma 1998;175:75–84.
34. Lin JJ, Wei JC, Tsai WC. Layered confinement of protein in synthetic fluorinated mica via stepwise polyamine exchange. J Phys Chem B 2007;111:10275–10280.
35. Vandenberg GW, Drolet C, Scott SL, de la Noüe J. Factors affecting protein release from alginate-chitosan coacervate microcapsules during production and gastric/intestinal simulation. J Control Release 2001;77:297–307.
36. Zhu S, Qian F, Zhang Y, Tang C, Yin C. Synthesis and characterization of PEG modified N-trimethylaminoethylmethacrylate chitosan nanoparticles. Eur Polym J 2007;43:2244–2253.